White Rose
university consortium
Universities of Leeds, Sheffield & York

eprints@whiterose.ac.uk
https://eprints.whiterose.ac.uk/

3rd Annual Conference in Energy Storage and Its Applications, 3rd CDT-ESA-AC,
11–12 September 2018, Sheffield, UK

Influence of physicochemical characteristics of carbon supports on Pd ethanol oxidation catalysts

Ahmed Elsheikh[a,b], Vitor L. Martins[c], James McGregor[a]

[a]Chemical and Biological Engineering Department, University of Sheffield, Mappin Street, Sheffield S1 3JD, UK
[b]Mechanical Engineering Department, South Valley University, ElMadares Street, Qena 83521, Egypt
[c] Depto. Química Fundamental, Instituto de Química, Universidade de São Paulo, Av. Prof. Lineu Prestes 748, 05508-000 São Paulo, SP, Brasil

Abstract

Direct ethanol fuel cells (DEFCs) have the potential to play a valuable role in the conversion of energy from sustainable sources. DEFCs need a support matrix, typically carbon, for the noble metal catalyst. In this work, two distinct carbon supports are compared and their electrochemical efficacy is related to their physicochemical characteristics. Specifically, Vulcan (C_v) is compared to Selectivity (C_s) as a support for Pd nanoparticles to catalyze ethanol electrooxidation. Characterisation data show that C_s has potentially favorable properties such as a high surface area. However, Pd/C_v exhibits a superior catalytic performance due to the higher adequacy of C_v texture that meets the particular needs of DEFC support in terms of pore size distribution. Additionally, synthesis of Pd nanoparticles on both carbons has decreased their surface areas and increased their pore sizes.

1. Introduction

Direct ethanol fuel cells could convert the ethanol chemical energy into electricity directly through the *redox* reactions occurring on the electrodes' surfaces. Each electrode contains a thin catalytic layer of the noble metal nanoparticles, support material, and binder [1]. The carbon used as a support for fuel cell electrocatalysts plays a crucial role in the catalytic performance of the electrode. It serves as a textural and mechanical support for the noble metal nanoparticles. Furthermore, it should be stable in acidic and alkaline environments in addition to the corrosion resistance it should have. Also, it provides high surface area for the dispersion for metal catalyst nanoparticles. Finally, it should be conductive electronically [2]–[4]. Carbon black with a mesoporous structure is of a great interest concerning these technical features. A commonly applied example is Vulcan carbon (C_v), which is mesoporous with a small fraction of micropores [3]. That means it has an adequate pore size (20 – 60 nm) facilitating the reactions in fuel cells while allowing enough space for the mass transfer of the reactants and products from electrocatalytic sites [5], [6]. Such

high pore size is necessary to accommodate the metal nanoparticles (5 -15 nm) and the micelles of the binder in the electrode catalytic layer. On the other hand, a high surface area is advantageous for better dispersion of the metal nanoparticles and increasing the catalytic sites [7], [8]. Therefore, choosing the best support should compromise among many factors and especially the surface area, pore size distribution, cost in addition to electronic conductivity and corrosion resistance.

This work investigates the impact of physicochemical and textural characteristics of two carbon supports on the electrochemical ethanol oxidation on Pd catalyst surface. While the surface area of Vulcan C_v is 220 – 250 m^2/g [3], it is 1,260 m^2/g for the Selectivity C_s [9].

2. Methodology

Chemicals were obtained from Sigma-Aldrich and were used as received. Two carbons, which are Vulcan (C_v) and selectivity (C_s), are obtained from Cabot Corp. The synthesis protocol follows polyol using the ethylene glycol as a solvent and reducing agent [10]. The required amount of metal precursor (4.415 mL, 0.128M) and each carbon (240 mg) were mixed separately and sonicated in 36 mL of ethylene glycol for 20 min. The Pd:C weight ratio is 20:80. Then, the pH was adjusted to 10 by adding 1M NaOH. Following, the catalysts' mixtures were stirred at 130˚C for 2.5 hours under reflux. Mixtures were, then, washed copiously with deionized water until neutralised. Finally, the wet powder was dried at 80˚C in a vacuum oven overnight. The Vulcan- and Selectivity-supported Pd catalysts are named Pd/C_v and Pd/C_s herein.

The catalyst structure is analysed by X-ray diffraction (XRD) using a Bruker D2 Phaser operating at 30 kV, 30 mA and 12º/min scan rate. The texture was examined by BET using a 3Flex Micrometrics Analyser at 77 K. The samples were degassed at 250ºC for 3 hours prior to BET. The metal concentration was quantified by inductive coupled plasma using a Spectro Ciros Vision ICP-ES. Then, electrochemical testing was performed using a 3-electrode half-cell in which the working electrode (WE) is a thin film of the catalyst powder, the reference electrode (RE) is Hg/HgO and the counter electrode (CE) is a Pt wire. The WE thin film was prepared by pipetting 20 µL from a mixture of the catalyst powder (5 mg), ethanol (1 mL), and Nafion (50 µL) on a glassy-carbon electrode, which was loaded 850 µg/cm^2. The Cyclic voltammetry, Chronoamperometry, and electrochemical impedance spectroscopy have been used to evaluate the electrochemical performance of both Pd/C_v and Pd/C_s. EIS was performed at constant potential of -0.2 vs Hg/HgO between 10,000 and 0.2 Hz.

3. Results and Discussion

The Pd metal concentration in each catalyst powder was quantified using ICP-ES which revealed 17.8% and 17.7% for Pd/C_v and Pd/C_s, respectively. *Fig. 1* shows the X-ray diffractinon patterns of both Pd/C_v and Pd/C_s. C_s has a more amorphus chachteristic than C_v informed from the intense broad peak at 25˚. The four other peaks are ascribed to the crystalline facets of Pd (111), (200), (220), and (311) at 40.56º, 46.6º, 68.1º, and 82.1º, respectively. The Pd peaks in case of Pd/C_s are obviously more intense than those of Pd/C_v whose peaks are much broader. The high extent of peak broadening in case of Pd/C_v is an evidence of a smaller crystal size than that of Pd/C_s. The crystal sizes of Pd/C_v and Pd/C_s were estimated using the Sherrer analysis to be 5.2 nm and 10.8 nm, respectively. The Pd shift for Pd/C_s suggests a lattice contraction has occurred during the synthesis of Pd/SC1. *Fig. 2* shows the textual analysis of Pd/C_s and Pd/C_v catalysts. Although Pd/C_s has a very high surface area (670 m^2/g) compared to Pd/C_v (182 m^2/g). Additionally, the pore size of Pd/C_s is 13 nm but that of Pd/C_v is 27 nm. This is interesting as the higher pore size of Pd/Cv assures there is more space surrounding the Pd nanoparticles to facilitate reactant/product mass transfer between the bulk solution and the electrode surface. While the microporous area of Pd/Cs is close to 300 m2/g, it is close to 15 m^2/g for Pd/Cv according to Fig. 2. That proves the micropores content in Pd/C_s is much more than Pd/C_v. It seems
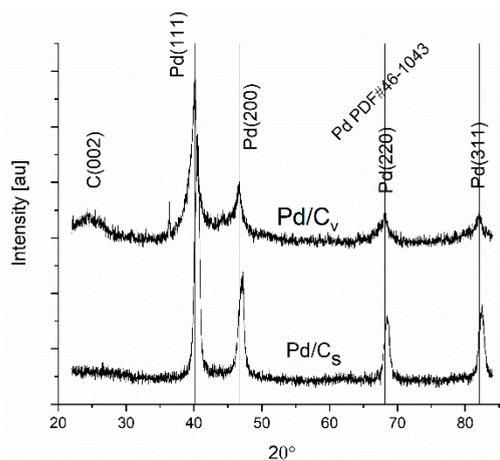
Fig. 1. X-ray diffraction pattern of Pd/C$_v$ and Pd/C$_s$

the Pd nanoparticles localised in the micropores and mesopores (<15 nm) of Pd/Cs are trapped in these internal small pores unlike Pd/C$_v$ whose micropores content is less than its content of larger mesopores (40 – 60 nm) as shown in Fig. 2. Further to that, the micropores area of raw C$_v$ measured in this work is 55 m^2/g while Martins et al. [9] has found that of C$_s$ equals 690 m^2/g. Therefore, it could be inferred the Pd nanoparticles are more exposed on the surface of C$_v$ than C$_s$.
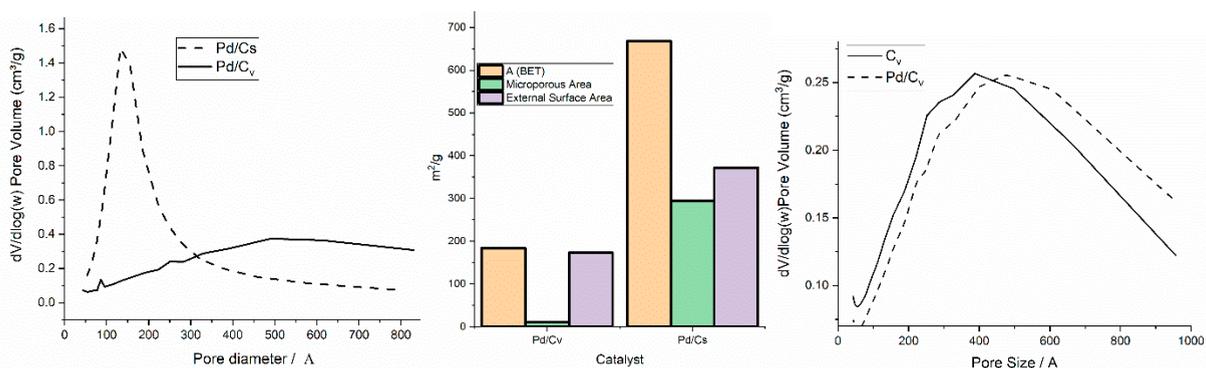

Fig. 2. BET particle size distribution of Pd/C$_v$, Pd/C$_s$ and C$_v$

Also, Fig. 2 compares the pore size distribution of the raw C$_v$ and C$_v$-supported Pd and a slight increase in the pore size is observed due to the interaction of Pd and C. The BJH desorption calculated pore sizes of C$_v$ and Pd/C$_v$ are 19 and 28 nm, respectively. Using analogy, it could be estimated the C$_s$ pore size is less than that of Pd/C$_s$, which is 13 nm and eventually the pore size of C$_s$ is highly probable to be less than 10 nm. Although the C$_v$ pore size increased after adding Pd to C$_v$, the opposite effect happened for the surface area, which has decreased from 230 m^2/g to 180 m^2/g. Similarly, the C$_s$ surface area dropped from 1260 m^2/g [9] to 670 m^2/g after preparing Pd/C$_s$.

Fig. 3 shows the cyclic voltamograms in 1M KOH of both catalysts. At -0.7 V, H is expected to be absorbed/desorbed from the catalyst surface and it could be seen form the higher current in case of Pd/C$_s$ (15 mA/mg$_{Pd}$) than Pd/C$_v$ that the former has a higher surface. The OH adsorption window is between -0.45 V and -0.1 V. The peaks observed between -0.4 V and -0.2 V in case of Pd/C$_v$ suggest more OH is adsorbed than Pd/C$_s$ which does not show a change in the current with increasing the potential. At around -0.1V, starts the surface layer oxidation of both catalysts which continues to the end of the forward scan. In the reverse scan, the PdO is reduced again -0.25 V. It is from the higher PdO reduction peak area in case of Pd/C$_v$ than Pd/C$_s$ that the former has a larger electrochemical active surface area even though Pd/C$_s$ has a much higher physical BET surface area. The electrochemical active surface area (EASA) is 45 and 18 m^2/g for Pd/C$_v$ and Pd/C$_s$, respectively. The cyclic voltamograms of both catalysts in 0.5M KOH + EtOH

is shown in Fig. 3, as well. As with the 1M KOH solution, the Pd/C has surpassed the Pd/C_s in terms of the catalytic activity for ethanol oxidation reaction (EOR). The reaction starts on Pd/C_v at -0.5 V while it starts at -0.4V on Pd/C_s which proves the former has a lower activation loss for EOR than the latter. In addition, the mass activity of Pd/C_v is 2.4 times as that of Pd/C_s looking at the oxidation current peak. Additionally, the forward/backward current ratio in case of Pd/C_v is more than that of Pd/C_s (an indicative of enhanced tolerance for poisoning species). The reasons for such enhanced performance are: 1. The smaller crystal size of Pd/C according to XRD measurement which indicates which explains the higher EASA of Pd/C_v compared to Pd/C_s (PdO reduction charge and real electrode surface area
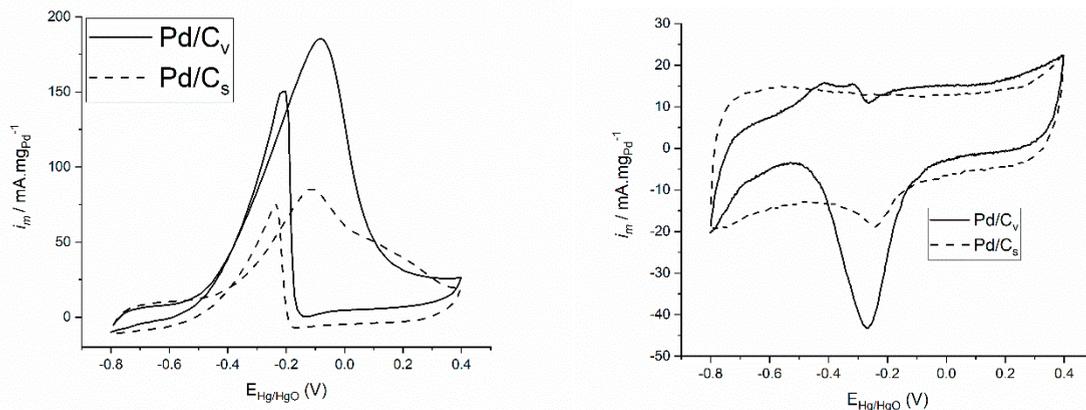

Fig. 3. Voltamograms of Pd/C_v and Pd/C_s in 1M KOH (left) and 0.5M KOH + EtOH (right), scan rate = 50 mV/s

are 3.67 mC and 9 cm^2 for Pd/C_v while they are 1.56 mC and 3.84 cm^2 for Pd/C_s), 2. The more suitable textural properties of Pd/C_v according to BET measurement, and 3. The higher degree of crystallinity of C_v than C_s according to XRD measurements. The higher crystallinity is expected to improve the order of Pd nanoparticles and make the interaction between the metal nanoparticles and support stronger [5,12]. Fig. 4 shows the chronoamperometry scans of Pd/C_v and Pd/C_s. It shows a higher current drawn using the Pd/C_v which substantiates the enhanced activity and tolerance for poisoning of Pd/C_v more than Pd/C_s for the previously mentioned reasons. Further to that the electrochemical impedance spectroscopy results are shown in the same figure.
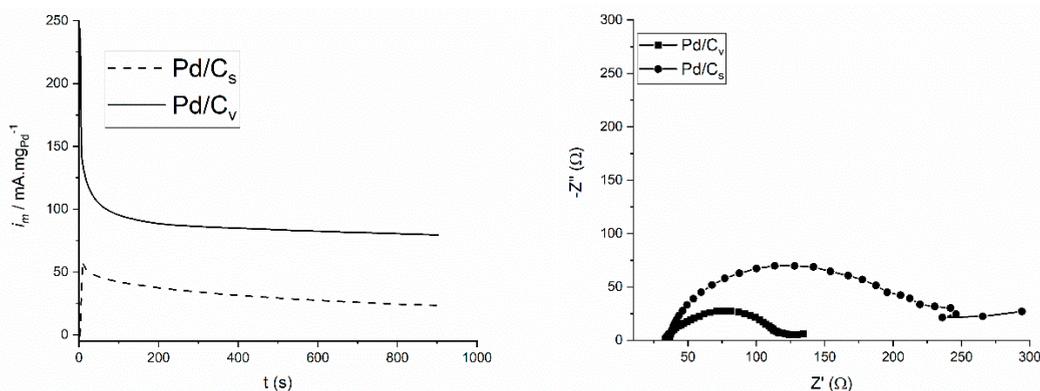

Fig. 4. Chronoamperometry (left) and EIS spectra (right) of Pd/C_v and Pd/C_s in 0.5M KOH + EtOH at -0.2V vs Hg/HgO

Due to the higher EASA and smaller crystal size of Pd/C_v compared to Pd/C_s, a better dispersion of Pd nanoparticles is anticipated on the C_v surface than C_s. Eventually, the number Pd electrocatalytic sites seems to be higher on Pd/C_v than Pd/C_s. The smaller impedance arc obtained with Pd/C_v than Pd/C_s suggests using the former would bring less charge transfer resistance between the electrode and solution. The less charge transfer resistance in case of Pd/C_v is a result of the higher number of active sites for EOR that are more difficult, to be blocked by poisons, than Pd/C_s.

4. Conclusions

The ethylene glycol reduction has been successful to prepare Pd nanoparticles supported on two carbons (Vulcan C_v and selectivity C_s). Preparing Pd nanoparticles has decreased the surface area and increased the pore size of both carbons. Despite the smaller physical surface area, Vulcan carbon has performed a better support role than selectivity one for ethanol electrooxidation on Pd. The reason behind is the more suitable textural and structural properties of Vulcan carbon.

Acknowledgements

References

[1]　A. Brouzgou, A. Podias, and P. Tsiakaras, "PEMFCs and AEMFCs directly fed with ethanol: A current status comparative review," *J. Appl. Electrochem.*, vol. 43, no. 2, pp. 119–136, 2013.

[2]　P. Kalyani and A. Anitha, "Biomass carbon & its prospects in electrochemical energy systems," *Int. J. Hydrogen Energy*, vol. 38, no. 10, pp. 4034–4045, Apr. 2013.

[3]　M. J. Lázaro, L. Calvillo, V. Celorrio, J. I. Pardo, S. Perathoner, and R. Moliner, "Study and application of Vulcan XC-72 in low temperature fuel cells," in *Carbon Black: Production, Properties and Uses*, no. May 2014, 2011, pp. 41–68.

[4]　R. L. McCreery, "Advanced carbon electrode materials for molecular electrochemistry," *Chem. Rev.*, vol. 108, pp. 2646–2687, 2008.

[5]　T. Ramulifho, K. I. Ozoemena, R. M. Modibedi, C. J. Jafta, and M. K. Mathe, "Fast microwave-assisted solvothermal synthesis of metal nanoparticles (Pd, Ni, Sn) supported on sulfonated MWCNTs: Pd-based bimetallic catalysts for ethanol oxidation in alkaline medium," *Electrochim. Acta*, vol. 59, pp. 310–320, 2012.

[6]　L. Calvillo, V. Celorrio, R. Moliner, and M. J. Lázaro, "Influence of the support on the physicochemical properties of Pt electrocatalysts: Comparison of catalysts supported on different carbon materials," *Mater. Chem. Phys.*, vol. 127, no. 1–2, pp. 335–341, May 2011.

[7]　E. L. Da Silva, M. R. Ortega Vega, P. D. S. Correa, A. Cuña, N. Tancredi, and C. D. F. Malfatti, "Influence of activated carbon porous texture on catalyst activity for ethanol electro-oxidation," *Int. J. Hydrogen Energy*, vol. 39, no. 27, pp. 14760–14767, 2014.

[8]　M. Carmo *et al.*, "Enhanced activity observed for sulfuric acid and chlorosulfuric acid functionalized carbon black as PtRu and PtSn electrocatalyst support for DMFC and DEFC applications," *Int. J. Hydrogen Energy*, vol. 36, no. 22, pp. 14659–14667, Nov. 2011.

[9]　V. L. Martins, R. M. Torresi, and A. J. R. Rennie, "Design considerations for ionic liquid based electrochemical double layer capacitors," *Electrochim. Acta*, vol. 270, pp. 453–460, Apr. 2018.

[10]　A. M. Sheikh, E. L. Silva, L. Moares, L. M. Antonini, M. Y. Abellah, and C. F. Malfatti, "Pd-based Catalysts for Ethanol Oxidation in Alkaline Electrolyte," vol. 2, no. 4, pp. 64–69, 2014.

[11]　T. Maiyalagan and K. Scott, "Performance of carbon nanofiber supported Pd–Ni catalysts for electro-oxidation of ethanol in alkaline medium," *J. Power Sources*, vol. 195, no. 16, pp. 5246–5251, Aug. 2010.

[12]　H. Rostami, A. A. Rostami, and A. Omrani, "An electrochemical method to prepare of Pd/Cu2O/MWCNT nanostructure as an anode electrocatalyst for alkaline direct ethanol fuel cells," *Electrochim. Acta*, vol. 194, pp. 431–440, Mar. 2016.